PAPER • OPEN ACCESS

Consolidation of memory traces in cultured cortical networks requires low cholinergic tone, synchronized activity and high network excitability

View the article online for updates and enhancements.

Journal of Neural Engineering

PAPER

Consolidation of memory traces in cultured cortical networks requires low cholinergic tone, synchronized activity and high network excitability

Inês Dias[1] , Marloes R Levers[1], Martina Lamberti[1], Gerco C Hassink[1], Richard van Wezel[2,3] and Joost le Feber[1,*]

[1] Department of Clinical Neurophysiology, University of Twente, Enschede, PO Box 217 7500AE, The Netherlands
[2] Department of Biomedical Signals and Systems, University of Twente, Enschede, PO Box 217 7500AE, The Netherlands
[3] Department of Biophysics, Radboud University, Nijmegen, PO Box 9010 6525AJ, The Netherlands
[*] Author to whom any correspondence should be addressed.

E-mail: j.lefeber@utwente.nl

Abstract

In systems consolidation, encoded memories are replayed by the hippocampus during slow-wave sleep (SWS), and permanently stored in the neocortex. Declarative memory consolidation is believed to benefit from the oscillatory rhythms and low cholinergic tone observed in this sleep stage, but underlying mechanisms remain unclear. To clarify the role of cholinergic modulation and synchronized activity in memory consolidation, we applied repeated electrical stimulation in mature cultures of dissociated rat cortical neurons with high or low cholinergic tone, mimicking the cue replay observed during systems consolidation under distinct cholinergic concentrations. In the absence of cholinergic input, these cultures display activity patterns hallmarked by network bursts, synchronized events reminiscent of the low frequency oscillations observed during SWS. They display stable activity and connectivity, which mutually interact and achieve an equilibrium. Electrical stimulation reforms the equilibrium to include the stimulus response, a phenomenon interpreted as memory trace formation. Without cholinergic input, activity was burst-dominated. First application of a stimulus induced significant connectivity changes, while subsequent repetition no longer affected connectivity. Presenting a second stimulus at a different electrode had the same effect, whereas returning to the initial stimuli did not induce further connectivity alterations, indicating that the second stimulus did not erase the 'memory trace' of the first. Distinctively, cultures with high cholinergic tone displayed reduced network excitability and dispersed firing, and electrical stimulation did not induce significant connectivity changes. We conclude that low cholinergic tone facilitates memory formation and consolidation, possibly through enhanced network excitability. Network bursts or SWS oscillations may merely reflect high network excitability.

1. Introduction

Network or population bursts are a widely observed phenomenon in neuronal ensembles. These patterns of synchronized activity occur during early brain development (Teppola *et al* 2019), certain sleep stages (Steriade and Timofeev 2003) and after various types of brain injury (Fardet *et al* 2018). Bursting patterns may have different functions: bursts might serve a specific purpose in neural development (Baltz *et al* 2010), in cognitive performance (Fries 2015), in information transfer (Lisman 1997) or it may be an epiphenomenon occurring whenever networks are insufficiently activated (le Feber *et al* 2010). Their role has mainly been speculated, with no evidence provided to support these hypotheses.

During slow-wave sleep (SWS), synchronous population discharges known as sharp waves, induce network bursts in region CA1 of the hippocampus (Miles and Wong 1983) and interact with oscillatory

rhythms as thalamo-cortical spindles (SPs) and slow oscillations (SOs), with their coupling believed to play a crucial role in memory consolidation (Axmacher *et al* 2006). After a newly acquired pattern has been formed as a result of the interaction between several structures within the medial temporal lobe, the encoded information is transferred to the neocortex where it is permanently stored, in a process known as systems consolidation (Axmacher *et al* 2006). In this stage of SWS, patterns are replayed by the hippocampus, which repeatedly activates neocortical areas (Atherton *et al* 2015). The oscillatory patterns observed during SWS coincide with low cholinergic tone in the neocortex and hippocampus (Drever *et al* 2011), whereas during the awake state these brain areas receive high cholinergic input (Hasselmo 1999). High acetylcholine (ACh) concentrations are thought to support memory encoding whereas low cholinergic tone is believed to potentiate memory consolidation (Gais and Born 2004). Despite the enormous oeuvre regarding systems consolidation during SWS, little is currently supported by experimental evidence (Queenan *et al* 2017). The underlying mechanisms of memory consolidation, as the roles of network bursts and cholinergic tone in both formation and consolidation of memory traces, are still a matter of debate. Limited accessibility to individual neurons and synapses of cortical networks and insufficient afferent input control are major difficulties that hamper high-quality experimental data collection *in vivo*.

In vitro models as dissociated cortical cultures plated on microelectrode arrays (MEAs) have been proposed as useful platforms to help resolve pending questions surrounding memory (Marom and Shahaf 2002, Dranias *et al* 2013). Networks of cortical neurons become active a week after plating, with spontaneous activity patterns including network bursts, periods of short intense firing synchronized on several electrodes (van Pelt *et al* 2004), which constitute the most striking display of spontaneous activity, although their function remains unclear. Networks reach a mature state three weeks after plating, when activity and connectivity stabilize (Wagenaar *et al* 2006). As activity patterns result from particular connectivity and specific patterns affect connectivity, it is suggested that networks develop a connectivity ⇔ activity balance where activity patterns support current connectivity (le Feber *et al* 2010). Without external input, this balance persists with minor fluctuations on time scales of hours to days (le Feber *et al* 2007). Electrical stimulation has been shown to disrupt this equilibrium and drive networks towards a new balance that includes the stimulus response in spontaneous activity patterns (le Feber *et al* 2015). Observed connectivity changes are interpreted as the formation of memory traces. These traces appear as network phenomena due to driving forces exposed on plastic networks, and are encoded by network connectivity.

In vivo, memory trace transfer to the neocortex through repeated replay by the hippocampus is referred to as systems consolidation. In the current study, we adhere to this commonly accepted terminology, and use the term systems consolidation to describe the formation and consolidation of memory traces in the cortex by repeated stimulation. When focussing at the cortex, as in the current study, systems consolidation is in fact equivalent to the induction and consolidation of memory traces.

Earlier work showed that repeated application of the same stimulus no further affected connectivity, suggesting stimulus memorisation. A second different stimulus induced connectivity changes when first exerted, but not upon subsequent application. Returning to the initial stimulus still did not affect connectivity, indicating that the second trace did not erase the first: parallel memory traces are consolidated (le Feber *et al* 2015).

These experiments consolidated memory traces in cortical cultures without cholinergic tone, and so activity patterns contained spontaneous network bursts comparable to patterns observed during SWS (Saberi-Moghadam *et al* 2018). To mimic the high cholinergic tone and absence of synchronized oscillations observed in the awake cortex, network bursts may be suppressed by mild activation, as regular dispersed firing decreases network excitability (the ease with which ongoing activity patterns induce synchronized bursting) (le Feber *et al* 2014). Combining the administration of a mild excitatory agent with repeated electrical stimulation may elucidate to which extent the formation and consolidation of a memory trace *in vitro* is influenced by the ongoing cholinergic tone.

We hypothesize that high cholinergic tone and absence of synchronized network bursts may hamper memory consolidation. To appraise the role of high network excitability and occurrence of bursting patterns, we electrically stimulated cortical networks receiving cholinergic input (through carbachol administration) or not, and analysed activity patterns and stimulus induced connectivity changes in both groups. We show that high cholinergic tone reduces network excitability and the occurrence of network bursts, impeding memory trace formation and consolidation.

2. Methods

2.1. Cell culturing

Cortical cells were obtained from Wistar rats at post-natal day 1. After neocortex isolation, cells were dissociated by trituration and trypsin treatment, and around 100 000 dissociated neurons (60 μl suspension) plated on a MEA (multi channel systems (MCS), Reutlingen, Germany; figure 1(A)), precoated with polyethyleneimine. This procedure led to an initial cell density of approximately
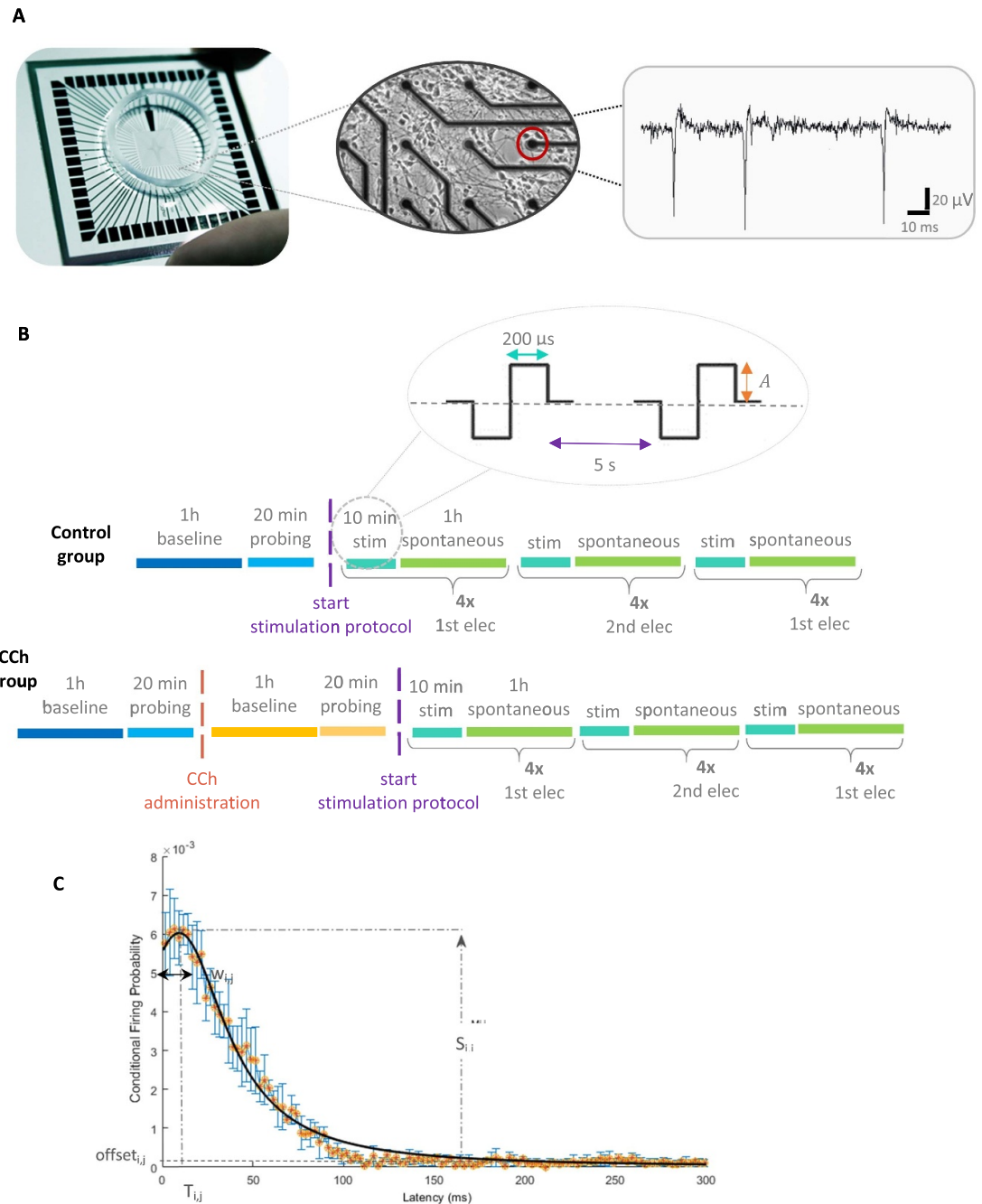
Figure 1. Microelectrode array (MEA), recorded activity, experimental design, stimulation pulses and conditional firing probability curves. (A) MEA, close up of a section of recording electrodes in contact with several neurons and an example of the spikes recorded at a single electrode. (B) Experimental design for the control (top scheme) and CCh groups (bottom scheme). In both groups, after recording 1 h of spontaneous activity (baseline), all electrodes were probed twice for each of the three predefined amplitudes (12, 24 and 36 μA) for 20 min, with the aim of choosing the amplitude (A) among the three tested and the two electrodes showing the clearest response to stimulation. In control cultures, the stimulation protocol began immediately after probing, with low-frequency pulses (200 μs per phase at a frequency of 0.2 Hz) applied through the first electrode for 10 min, followed by a 1 h period of no stimulation. These two blocks were repeated four times for the first electrode. When finished, stimulation through the second selected electrode was applied with the same paradigm and finally, the first electrode was again used to stimulate the network. In CCh-treated cultures, carbachol was administered to the bath after probing, with a second 1 h of baseline and 20 min probing procedure after pharmacological manipulation. The same stimulation paradigm described for controls was then applied to CCh cultures. (C) Probability curve (equation (2)) fitted to activity recorded from a pair of active electrodes (i,j) in a control culture. The solid black line represents the fitted function, used to obtain the values for the strength ($S_{i,j}$, maximum of the curve above offsert) and latency ($T_{i,j}$, time until maximum is reached) of functional connections. $w_{i,j}$ is the width of the distribution peak (black arrow), and offset$_{i,j}$ reflects uncorrelated background activity. Figure (C) has been reproduced from (le Feber *et al* 2007). © IOP Publishing Ltd. All rights reserved.

5000 cells mm^{-2}, which gradually decreased to approximately 2500 cells mm^{-2} by the time of the experiments (26 ± 6 d). Cultures contained neurons and astrocytes (le Feber *et al* 2017). The presence of excitatory and inhibitory neurons has been confirmed electrophysiologically (le Feber *et al* 2016) and immunohistochemically (le Feber *et al* 2018). At 18–22 d *in vitro* (DIV), approximately 53% of all synapses were excitatory. Cells were cultured in a circular chamber with inner diameter $d = 20$ mm, glued on top of a MEA with 60 titanium nitride electrodes (30 μm diameter and 200 μm pitch). The culture chamber was filled with ∼700 μl R12 medium. MEAs were stored in an incubator under standard conditions of 36 °C, high humidity and 5% of CO_2 in air. The medium was changed twice a week. After each experiment, the cultures were returned to the incubator. We used 23 cultures in 23 experiments, which were performed 26 ± 6 d after plating (culture age ranged from 19 to 36 d *in vitro*). Cultures used were considered to be in the mature phase of development, when network bursting patterns dominated spontaneous activity (van Pelt *et al* 2004). We will refer to 'bursting' as synchronicity of firing across the cell culture, and not bursting in a single neuron. All surgical and experimental procedures complied with Dutch and European laws and guidelines (AVD110002016802).

2.2. Recording set-up

For recording, cultures were placed in a measurement set-up outside the incubator. Signals from 59 MEA-channels were recorded at a sampling frequency of 16 kHz, with noise levels typically from 3 to 5 μV_{RMS}. Culture chambers were firmly sealed with watertight but O_2 and CO_2 permeable foil (MCS; ALA scientific) and the temperature was kept at 36 °C. During recordings, the measurement setup was placed under a Plexiglas hood that received a constant flow (2 l min^{-1}) of a humidified gas mixture that contained 5% CO_2. Recordings began after a 20 min accommodation period. A custom-made LabView application was used for data acquisition, with all analogue signals band-pass filtered (0.1–6 kHz) before sampling. Due to their size, recording electrodes might have been in contact with several units, and the activity recorded may reflect single action potentials or multi-unit activity. Therefore, we will refer to the recorded signals by the term 'spike'. Candidate spikes were detected whenever signals crossed the detection threshold, set at 5.5 times the estimated root-mean-square noise level. This threshold was continuously updated for each electrode throughout the duration of recordings. Time stamps, electrode numbers, and 6 ms of wave shapes (figure 1(A)) were stored for each candidate spike. Stored wave shapes were used for off-line artefact detection and removal as in (Wagenaar *et al* 2005). A candidate spike was considered valid if: (a) no other peaks with equal or

higher amplitude were recorded within a 1 ms window around the main peak of the waveform; (b) no other peaks with the same polarity and more than 90% of the amplitude of the candidate spike existed within a 0.3 ms window around the peak; and (c) no other peaks with the same polarity and more than 50% of the amplitude of the candidate spike existed within a 1 ms window around the peak. These thresholds are used to reduce the rate of false positive detections. All cultures were tested for bursting patterns a day prior to the beginning of each experiment and 30 min before baseline recordings. Cultures were included for analysis only if summed activity of all electrodes was at least 2500 spikes per 5 min of spontaneous activity (le Feber *et al* 2007). Spike sorting was not used in this study, as the reliability of this waveshape based technique is disputed, in particular because the waveshapes of action potentials may substantially change, e.g. during bursting (Lewicki 1998, Sukiban *et al* 2019). Consequently, we used activity of very small subsets of neurons as the unit of activity, rather than activity of individual neurons.

2.3. Disruption of network bursts

ACh has been shown to modulate connection strength and neural synchronization events (Colangelo *et al* 2019). Although the effects of ACh on cortical functioning strongly depend on concentration (Drever *et al* 2011), this value is hard to determine *in vivo*. Early microdialysis studies reported concentrations as low as 0.1–6 nM in the cortex of awake rodents (Gil *et al* 1997, Pasquale *et al* 2008). However, ACh is rapidly hydrolysed after its release in the synaptic cleft, which probably causes underestimation of the effective concentration, and so approaches such as magnetic resonance spectroscopy (MRS) have been proposed to tackle this issue (Turrigiano and Nelson 2000, Turrigiano 2010). MRS targets extracellular choline, which is both a precursor of ACh and a metabolite of its hydrolysis (Bell *et al* 2018). In the choline cycle, the re-uptake of this metabolite by the pre-synaptic cell is not as fast as the hydrolysis of ACh, increasing the measurable concentration (Bell *et al* 2018). Several studies reported choline concentrations of 1–5 mM in the cortex of healthy volunteers and 0.6–13 μM in the cortex of awake rat and mice, with a proportional correlation between choline and ACh concentrations (Gil *et al* 1997, Turrigiano and Nelson 2000, Pasquale *et al* 2008, Yger and Gilson 2015).

Carbachol, a synthetic derivative of choline and a selective cholinergic agonist, was observed to have comparable desynchronization effects as ACh at medium concentrations (Tateno *et al* 2005). In contrast to ACh, carbachol is resistant to hydrolysing enzymes, remaining present in the culture medium for several hours (le Feber *et al* 2014). Carbachol (CCh, Sigma-Aldrich, St. Louis, MO, USA), was prepared in a stock solution of 400 μM in phosphate

buffered saline and applied in half of all cultures, aiming to supress naturally occurring bursts. To determine the carbachol concentration needed for this suppression 5, 10, 20, and 40 μM CCh were tested in three spontaneously bursting cultures (35 ± 3 DIV). CCh in this concentration range was found to disrupt network bursts in earlier studies (Tateno *et al* 2005, le Feber *et al* 2014). After a 30 min baseline recording of spontaneous activity, CCh was increased in a stepwise manner, with 30 min recordings of spontaneous activity following each increase, used to quantify network bursting. We determined the sustainability of the burst suppressing effect during 15 h recordings in four spontaneously bursting cultures (30 ± 5 d *in vitro* (DIV)).

2.4. Electrical stimulation

We applied low frequency stimulation at 0.2 Hz in all cultures (figure 1(B)). Stimuli consisted of biphasic rectangular current pulses (200 μs per phase, negative phase first). Only 59 electrodes of each MEA were used for stimulation and signal recording, as electrode 15 was set as reference. To determine suitable electrodes and pulse amplitudes for stimulation, first stimulation was applied to all 59 electrodes twice using three different pulse amplitudes (12, 24, and 36 μA), in a pseudo random order after the baseline recording of experiments. The two electrodes showing the clearest stimulus response, with latencies between 20 and 100 ms, were subsequently used for the stimulation protocol. Amplitudes were set to 24 or 36 μA, such that typically more than 50% of the stimuli triggered a network response (synchronous activity in most of the network during 100–200 ms following the stimulus) but still avoided high voltage induced electrolysis at the electrodes.

2.5. Experimental design

We explored the effects of carbachol administration and repeated electrical stimulation on the activity and connectivity of 23 dissociated cortical cultures. Thirteen cultures (25 ± 6 DIV) were randomly assigned to the control group while the remaining 10 (27 ± 6 DIV) were treated with CCh. Three cultures were excluded from the control group after the recordings, due to abnormal activity caused by a bacterial infection or a data storage problem during recording. In the CCh group, two cultures were excluded for not meeting the inclusion criteria (mean firing rate (MFR) < 2500 spikes/5 min, see subsection section 2.6). The final sample sizes consisted of $n = 10$ controls (non-CCh treated cultures) and $n = 8$ CCh-cultures (treated cultures). The total duration of experiments was kept at or just below 15 h, aiming to avoid spontaneous connectivity changes (le Feber *et al* 2007, 2010). In both groups, experiments consisted of a 1 h baseline recording, followed by electrode probing to select stimulation electrodes (as described in

the subsection section 2.4). Figure 1(B) illustrates the experimental procedure.

In control cultures, the stimulation protocol started immediately after probing. Low-frequency pulses were applied through the first selected electrode for 10 min, followed by a 1 h period of no stimulation. This period of spontaneous activity recording allowed to infer on functional connectivity. Each 10 min stimulation epoch and the subsequent 1 h of spontaneous activity block were repeated four times. When finished, stimulation through the second selected electrode was applied with the same paradigm. Finally, the first electrode was again used to stimulate the network in the same fashion (figure 1(B)).

CCh administration in the CCh-group occurred after the initial probing. In this group, another 1 h baseline recording was followed by a second probing procedure, prior to the beginning of the stimulation protocol as described for control cultures (four periods of stimulation in each electrode, separated by 1 h periods of no stimulation; figure 1(B)).

2.6. Data analysis

Recorded data were analysed in terms of activity, connectivity and network excitability. All data analysis was performed in MATLAB R2018a (MathWorks, Massachusetts, USA). As already stated, recorded signals may reflect multi-unit activity, so we will refer to the activity of and relationships between MEA electrodes, rather than neurons.

Several outcome measures were derived: firing patterns were characterized by the raster plot, the MFR, the burstiness index (BI) and the post-stimulus time histogram (PSTH); functional connectivity was assessed through conditional firing probabilities (CFPs) and connectivity changes by Euclidian distances between connectivity matrices; finally, network excitability was quantified through mean single pulse responses' (SPRs) strengths.

Regarding activity measures, a raster plot depicts the activity of a group of neurons recorded by each MEA electrode, with the *y*-axis displaying the activity recorded in each channel over time (*x*-axis). Each tick in the graph corresponds to a spike detected by a particular electrode at the corresponding time stamp. The MFR was computed as defined by (Bologna *et al* 2010). In short, the firing rate of each single channel was firstly obtained as the number of recorded spikes per hour in 1 h bins. FRs were averaged across all active electrodes of the MEA, to obtain the MFR. Electrodes were considered active if more than 200 spikes were recorded at that channel in that 1 h bin. BI (Wagenaar *et al* 2005) was used to quantify the synchronicity of each culture. Briefly, each 5 min of a recording were divided into 300-time bins of 1 s each, with the number of spikes across all electrodes counted in each bin. Then the fraction of spikes accounted for by the 15% of bins with the largest spike counts, f_{15}, was computed.

BI was calculated as a normalized measure between 0 and 1:

$$BI = \frac{f_{15} - 0.15}{0.85}. \tag{1}$$

BI values close to 1 reflect burst dominated activity patterns, whereas a BI equal to 0 indicates absence of bursts. PSTH were computed per stimulation period for all stimuli, showing the summed number of recorded spikes of all electrodes in 5 ms bins recorded during the interval 300 ms before until 300 ms after the stimulus. For each stimulation electrode, responses to individual stimuli were summed to obtain that electrodes' PSTH. The area under PSTH curves between 5 and 300 ms post-stimulation was computed per stimulation epoch, to detect any trend in the effectiveness of stimulation during experiments. Background activity after stimulus onset was removed by subtraction of the area under the curve as present prior to stimulation, to allow for comparison between the effect of stimulation in both control and CCh group.

Functional connectivity was analysed by pairwise estimation of CFPs, and changes in functional connectivity were assessed by Euclidian distances between connectivity matrices. We adapted the procedure described by le Feber *et al* (2007) to estimate CFPs. Baseline and spontaneous activity epochs recorded between stimulation periods were divided in data blocks of 2^{13} recorded spikes. This block size was chosen such that all epochs contained multiple data blocks in all experiments. We chose to divide recordings into data blocks that contained a fixed number of spikes (summed across all electrodes) instead of blocks with fixed duration to avoid large fluctuations in the amount of activity between data blocks. In blocks with fewer spikes, connections between electrodes that do not reach the activity threshold may remain undetected, which would affect connectivity estimates. CFPs were estimated for all possible pairs of active electrodes by the relative occurrence of a spike at electrode j at latency τ (in 0.5 ms bins; $0 < \tau < 500$ ms), after i fired at $t = 0$. A four-parameter function was fitted to the obtained curve:

$$CPF_{i,j}^{fit}[\tau] = \frac{S_{i,j}}{1 + \left(\frac{\tau - T_{i,j}}{w_{i,j}}\right)^2} + offset_{i,j} \tag{2}$$

in which $S_{i,j}$ is the maximum above offset that represents the strength of a connection, $T_{i,j}$ its latency, $w_{i,j}$ the width of the distribution peak, and $offset_{i,j}$ the offset level, which reflects unrelated background activity (figure 1(C)). Electrodes that recorded >200 spikes within a data block were considered active, a value slightly adapted from previous work (le Feber *et al* 2007), to account for the fewer spikes per data block, and still ensure a sufficient number of data

points to fit equation (2). If a CFP distribution was not flat ($S_{i,j} > offset_{i,j}$; $T_{i,j} < 250$ ms; $w_{i,j} < 250$), the two electrodes were considered functionally connected (figure 1(C)). If at least one of these criteria was not met, the connection strength was set to $S_{i,j} = 0$. The average number of functional connections ($N = |\{S_{i,j} > 0\}|$) was counted before and after CCh administration as well as the number of connections existing prior to the stimulation protocol and after its completion. The strengths of all connections calculated through the CFPs were combined into a connectivity matrix S for each data block. These matrices were used to monitor the evolution of connectivity throughout the different phases of experiments. To assess the magnitude of changes between subsequent data blocks, the Euclidian distance (ED_0) between connectivity matrices at time t and time t_0 can be expressed as

$$ED_0(t) = \sqrt{\sum_{i=1}^{n}\sum_{j=1}^{a}\left[S_{ij}(t) - S_{ij}(t_0)\right]^2} \tag{3}$$

with $t > t_0$. In the case of baseline recordings, t_0 was chosen as the first data block of the recording, while in the case of stimulation at each electrode, t_0 was chosen as the last data block before stimulation at that specific electrode. Only non-zero elements of connectivity matrices ($S(t_0)$ as well as $S(t)$) were considered in equation (3). ED_0 values were normalized ($ED_{0,\,norm}$) to the mean strength of all connections in the data block chosen for t_0 and averaged for each 1 h of spontaneous activity. These values were compared with baseline connectivity. The distance between the connectivity before and after a stimulation period (ED_{stim}) was calculated using equation (3) but choosing t_0 as the last data block separated from t by a stimulation period. ED_{stim} values were normalized to the mean strength of all connections in the data block chosen for t_0 and averaged for each 1 h of spontaneous activity. These values were compared with $ED_{baseline}$, which corresponds to the mean distance between subsequent connectivity matrices during baseline. $ED_{baseline}$, values were normalized to the mean strength of all connections in the 1 h baseline period.

To quantify network excitability (the average neural network response to a spike in one neuron), we calculated SPRs, following the approach presented in le Feber *et al* (2014). SPRs enable estimation of the average response at electrode j to a single spike at electrode i under widely varying dynamic regimes, and are calculated by deconvolving the autocorrelation of electrode i from $CFP_{i,j}$. Spontaneous activity recordings were subdivided into data blocks of 2^{13} recorded spikes, the same block size as used for the CFP analysis. Mean SPR strengths of all pairs of active electrodes were calculated for control and CCh groups
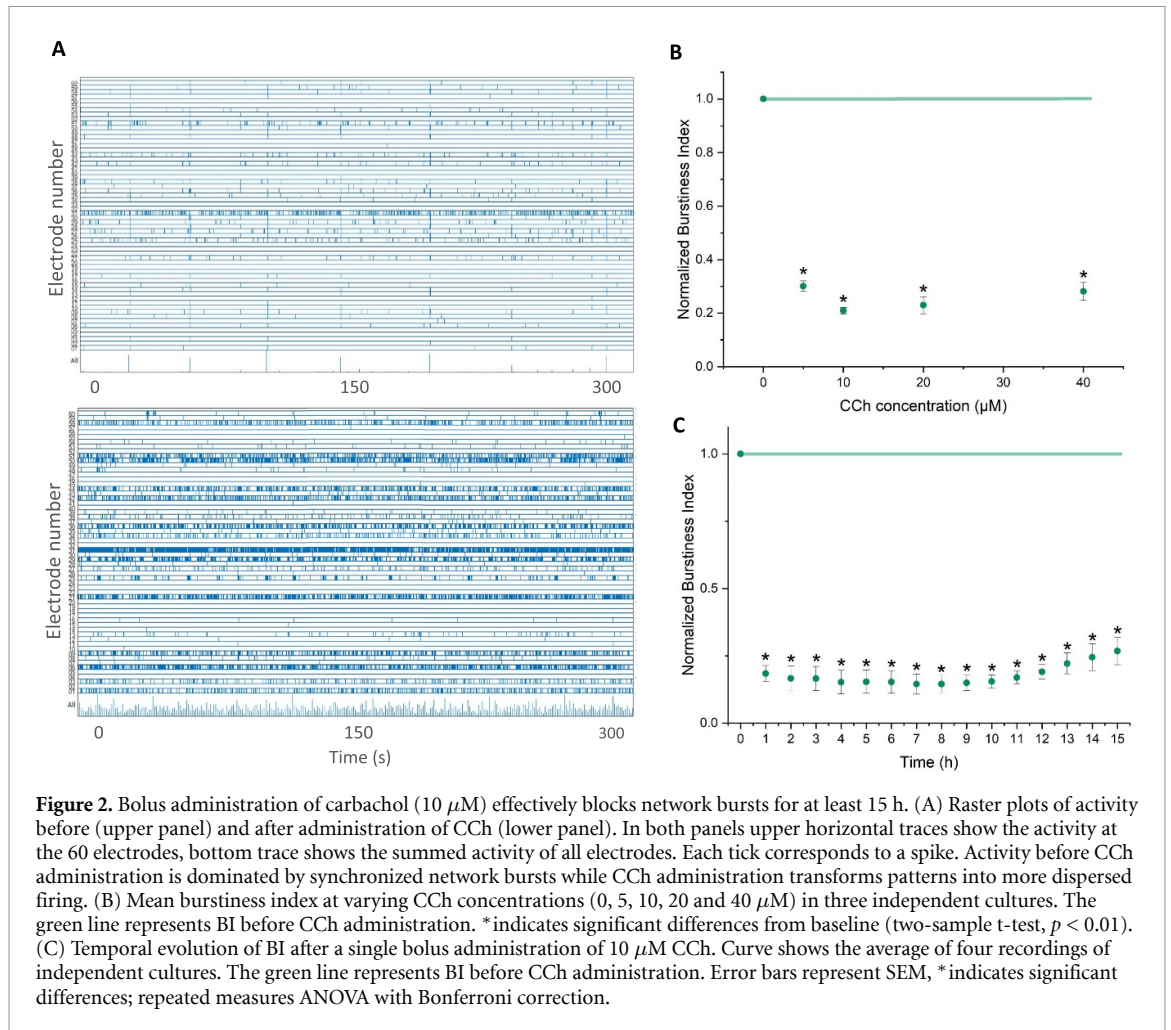
Figure 2. Bolus administration of carbachol (10 μM) effectively blocks network bursts for at least 15 h. (A) Raster plots of activity before (upper panel) and after administration of CCh (lower panel). In both panels upper horizontal traces show the activity at the 60 electrodes, bottom trace shows the summed activity of all electrodes. Each tick corresponds to a spike. Activity before CCh administration is dominated by synchronized network bursts while CCh administration transforms patterns into more dispersed firing. (B) Mean burstiness index at varying CCh concentrations (0, 5, 10, 20 and 40 μM) in three independent cultures. The green line represents BI before CCh administration. *indicates significant differences from baseline (two-sample t-test, $p < 0.01$). (C) Temporal evolution of BI after a single bolus administration of 10 μM CCh. Curve shows the average of four recordings of independent cultures. The green line represents BI before CCh administration. Error bars represent SEM, *indicates significant differences; repeated measures ANOVA with Bonferroni correction.

to quantify and compare network excitability under both conditions.

2.7. Statistical analysis

All results are shown as the mean and standard error of the mean (SEM). Statistical testing was performed in SPSS (IBM, New York, USA) and Origin2019 (OriginLab, Massachusetts, USA), with a significance level of 5%. The homogeneity of variances and the normal distribution of the residuals were assessed using Levene's test with 5% significance, a Shapiro–Wilk test, and Q–Q plots. If the data were normally distributed, two-sample t-tests, one-way repeated measures ANOVA or two-way repeated measures ANOVA were applied. A Wilcoxon test was applied in case of non-normally distributed data. In case of multiple pair-wise comparisons, we manually corrected the significance threshold using Bonferroni correction. Various analyses involved 4, 12 or 15 repetitions, yielding Bonferroni corrected significance thresholds of $p < 0.0125$ (figures 5(B) and (C)), $p < 0.0042$ (figures 3(A), (B) and 5(A)) or $p < 0.0033$ (figure 2(C)), respectively. Each test is presented with the corresponding p-value (in case of significance, the largest p-value from all pairwise comparisons is

reported, and in case of non-significance, the smallest value is reported).

3. Results

3.1. Carbachol blocks network bursting throughout the 15 h of experiments

The carbachol concentration necessary to alter the natural synchronicity of dissociated cortical cultures was assessed by applying accumulating CCh concentrations to the culture bath in three independent cultures at 35 $\pm$ 3 DIV. Figure 2(A) displays raster plots of spontaneous activity recorded in of one of the cultures tested before pharmacological excitation (upper panel), and after 10 μM of CCh (lower panel). At all concentrations tested, carbachol enhanced activity and transformed patterns from burst dominated into more dispersed firing (figure 2(B)). Consequently, BI significantly decreased (two-sample t-test, $p < 0.01$). Lowest BI (0.21 ± 0.01) was reached after the administration of 10 μM of CCh.

We used four spontaneously bursting cultures (30 $\pm$ 6 DIV) to verify that the pattern alteration induced by a single bolus administration of 10 μM CCh persisted for at least the 15 h duration
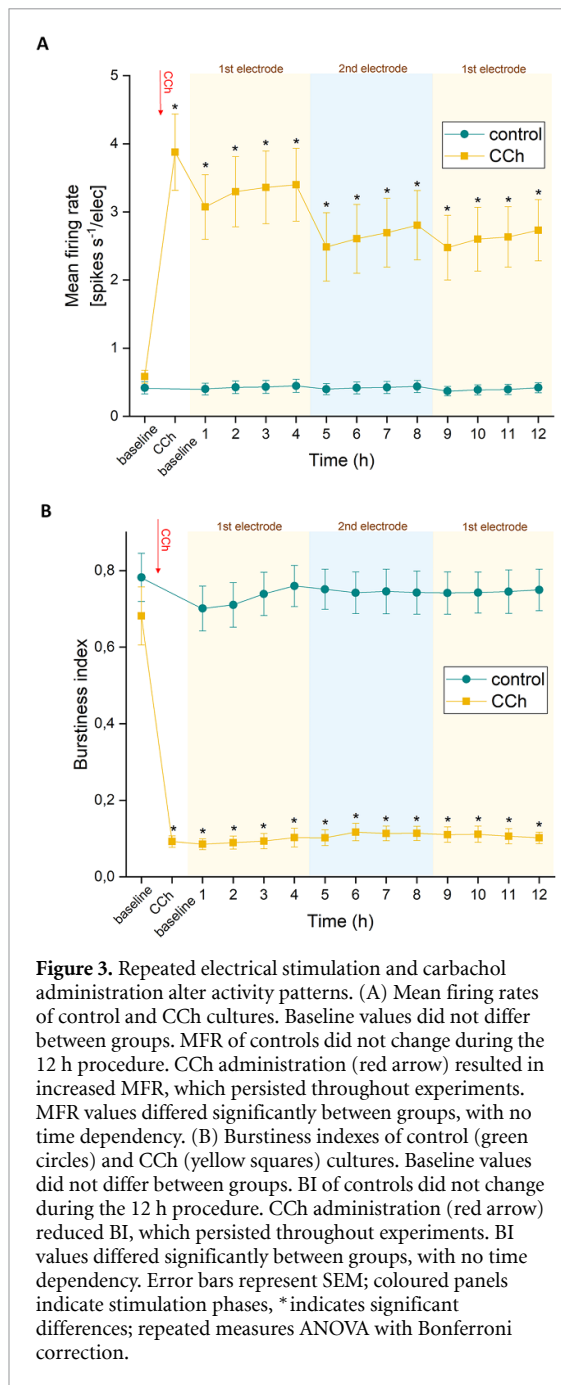
Figure 3. Repeated electrical stimulation and carbachol administration alter activity patterns. (A) Mean firing rates of control and CCh cultures. Baseline values did not differ between groups. MFR of controls did not change during the 12 h procedure. CCh administration (red arrow) resulted in increased MFR, which persisted throughout experiments. MFR values differed significantly between groups, with no time dependency. (B) Burstiness indexes of control (green circles) and CCh (yellow squares) cultures. Baseline values did not differ between groups. BI of controls did not change during the 12 h procedure. CCh administration (red arrow) reduced BI, which persisted throughout experiments. BI values differed significantly between groups, with no time dependency. Error bars represent SEM; coloured panels indicate stimulation phases, *indicates significant differences; repeated measures ANOVA with Bonferroni correction.

of experiments (figure 2(C)). CCh administration significantly reduced BI (repeated measures one-way ANOVA, $p < 0.001$) throughout the 15 h recording procedure. In further experiments, 10 μM CCh was used to suppress bursting in cultures that were electrically stimulated for memory trace induction.

3.2. Repeated electrical stimulation and carbachol administration alter activity patterns but not stimulus responses

We analysed spontaneous activity, connectivity and excitability in ten control (24 ± 5 DIV) and eight CCh cultures (28 ± 6 DIV). Figure 3(A) shows the temporal evolution of the MFR in control and CCh cultures. Baseline MFR (0.42 ± 0.09 (control) and
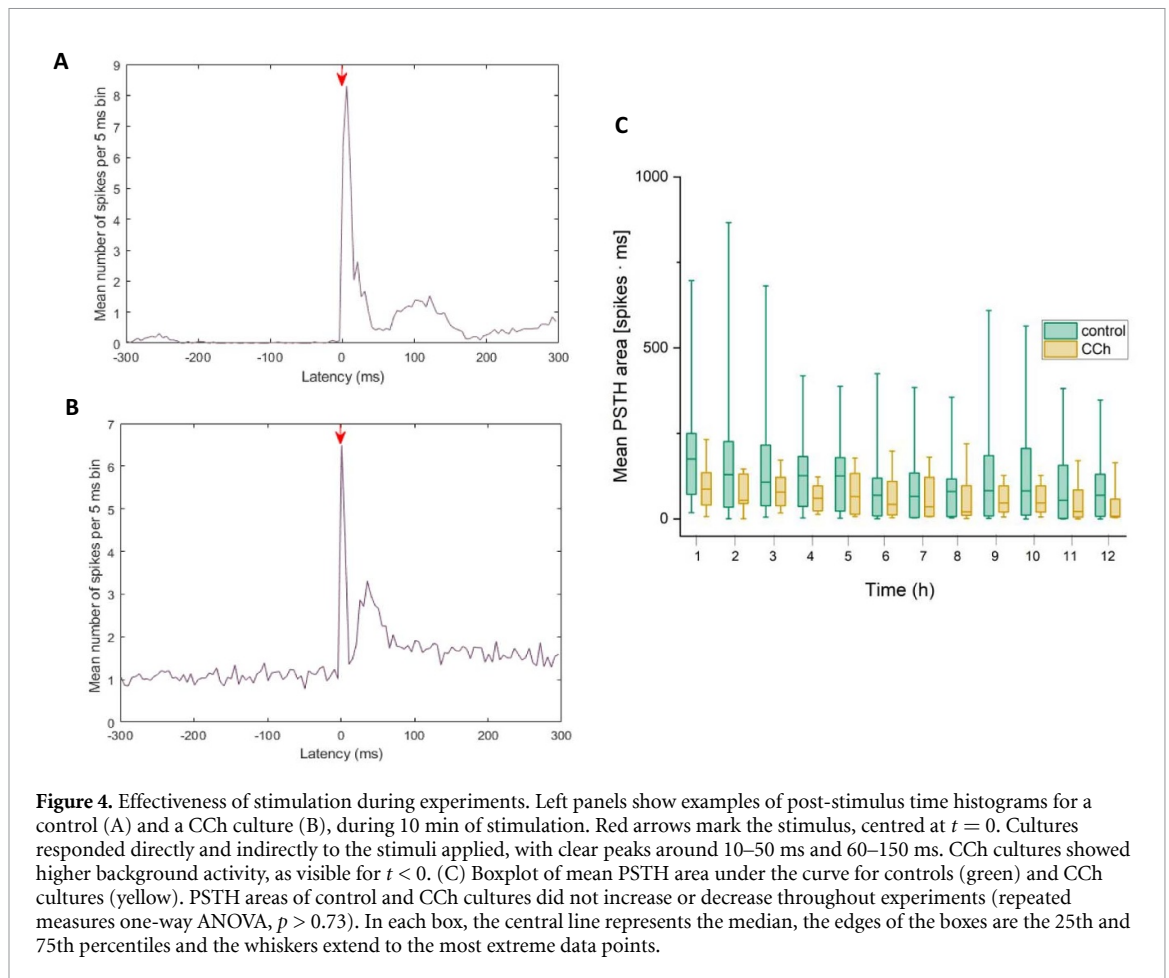
0.58 ± 0.09 spikes s^{-1} (Hz) per electrode (CCh)) did not differ significantly between groups (two sample t-test, $p > 0.22$). The MFR of control cultures remained rather constant around this baseline value, with no significant alterations during the 12 h procedure (repeated measures one-way ANOVA, $p > 0.14$). In CCh cultures MFR significantly increased immediately after carbachol administration (repeated measures one-way ANOVA, $p < 0.003$), and became significantly higher than in control cultures (two-way repeated measures ANOVA, $p < 0.001$). This effect did not fade with time (two-way repeated measures ANOVA, $p > 0.60$).

Mean BI values (figure 3(B)) at baseline for the control (BI = 0.78 ± 0.06) and CCh groups (0.68 ± 0.08) did not significantly differ (two sample t-test, $p > 0.32$). Baseline BI values were maintained throughout the duration of experiments in control cultures (repeated measures one-way ANOVA, $p > 0.12$). In carbachol-treated cultures, BI values dropped significantly in the 1 h baseline period after CCh administration to 0.09 ± 0.02 (repeated measures one-way ANOVA, $p < 0.001$), and remained around this value during the remainder of experiments. BI was significantly lower in CCh cultures than in control cultures (two-way repeated measures ANOVA, $p < 0.001$), with no effect of time on the differences observed (two-way repeated measures ANOVA, $p > 0.77$).

Figure 4 shows typical examples of PSTH curves obtained during a 10 min stimulation period. In a control culture (figure 4(A)), PSTHs showed almost no background activity before and after stimulus onset at $t = 0$. CCh-treated cultures showed similar PSTHs (figure 4(B)), but with enhanced background activity. Figure 4(C) shows the mean temporal evolution of areas under the PSTH curves of control and CCh cultures. These did not significantly differ from each other and showed no significant trend during the 12 h of recordings (two-way repeated measures ANOVA, $p > 0.73$).

3.3. Connectivity changes require high connection strength, low cholinergic input and mainly occur during the first stimulation period in each electrode

To infer on functional connectivity, we computed a CFP for each pair of active electrodes *(i,j)* per culture. Most active electrode pairs in control and CCh cultures (approximately 70%) displayed a non-flat curve (figure 1(D)), and parameters of equation (2) were fitted, i.e. offset (uncorrelated background activity), S (peak height above offset, interpreted as connection strength), T (latency until maximum CFP), and width (peak-width at 80% height). Baseline recordings in control cultures contained (5 ± 4) data blocks, whereas baseline recordings after CCh treatment contained (30 ± 24) data blocks on average. The total number of functional connections during baseline

Figure 4. Effectiveness of stimulation during experiments. Left panels show examples of post-stimulus time histograms for a control (A) and a CCh culture (B), during 10 min of stimulation. Red arrows mark the stimulus, centred at $t = 0$. Cultures responded directly and indirectly to the stimuli applied, with clear peaks around 10–50 ms and 60–150 ms. CCh cultures showed higher background activity, as visible for $t < 0$. (C) Boxplot of mean PSTH area under the curve for controls (green) and CCh cultures (yellow). PSTH areas of control and CCh cultures did not increase or decrease throughout experiments (repeated measures one-way ANOVA, $p > 0.73$). In each box, the central line represents the median, the edges of the boxes are the 25th and 75th percentiles and the whiskers extend to the most extreme data points.

did not differ significantly between control (173 ± 25 connections) and CCh cultures (132 ± 23 connections) (two-sample t-test, $p > 0.32$), and average connection strengths did not differ between groups (two-sample t-test, $p > 0.22$). Figure 5(A) shows the temporal evolution of connection strengths for control and CCh cultures. In control cultures, the average connection strength (10^{-3}–10^{-2}) remained rather constant throughout experiments (repeated measures one-way ANOVA, $p > 0.12$), whereas CCh administration immediately led to significantly lower connection strengths (10^{-4}–10^{-3}; repeated measures one-way ANOVA, $p < 0.002$), which then remained unaffected throughout the remaining 12 h of experiments (repeated measures one-way ANOVA, $p > 0.25$). Upon CCh administration, the average number of functional connections slightly tended to decrease compared to numbers before manipulation (two-sample t-test, $p > 0.84$).

To assess the magnitude of connectivity changes induced by stimulation at a particular electrode, we computed normalized Euclidian distance values ($ED_{0,norm}$) between mean baseline connectivity and connectivity matrices obtained for each 1 h of spontaneous activity (figure 5(B)). $ED_{0,norm}$ values during baseline did not significantly differ between the control and the CCh group before CCh administration (two-sample t-test, $p > 0.24$) nor after (two-sample

t-test, $p > 0.79$). Stimulation yielded a significant increase in $ED_{0,\,norm}$ in the control group (repeated measures one-way ANOVA, $p < 0.01$), with a larger distance between the connectivity before and after the first stimulation period than between subsequent stimulation periods. Switching to a second stimulation electrode again yielded larger distances between connectivity matrices separated by the first stimulation period, with non-significant differences between subsequent stimulation periods (repeated measures one-way ANOVA, $p > 0.22$). Stimulating the cultures again with the first electrode no longer induced significant connectivity changes (repeated measures one-way ANOVA, $p > 0.17$). The effect of stimulation was strikingly different in CCh-treated cultures, in which we did not observe any significant connectivity changes throughout the experiment (repeated measures one-way ANOVA, $p > 0.62$).

To assess the magnitude of changes between the connectivity before and after a stimulation period, we computed normalized ED_{stim} values around each stimulation period (figure 5(C)). We also calculated Euclidean distances between subsequent connectivity matrices obtained during baseline, $ED_{baseline}$. For control cultures, the distance between the connectivity before and after the first stimulation periods on the initial stimulation electrode was larger than ED_{stim} around later stimulation periods, $ED_{stim}[1]$
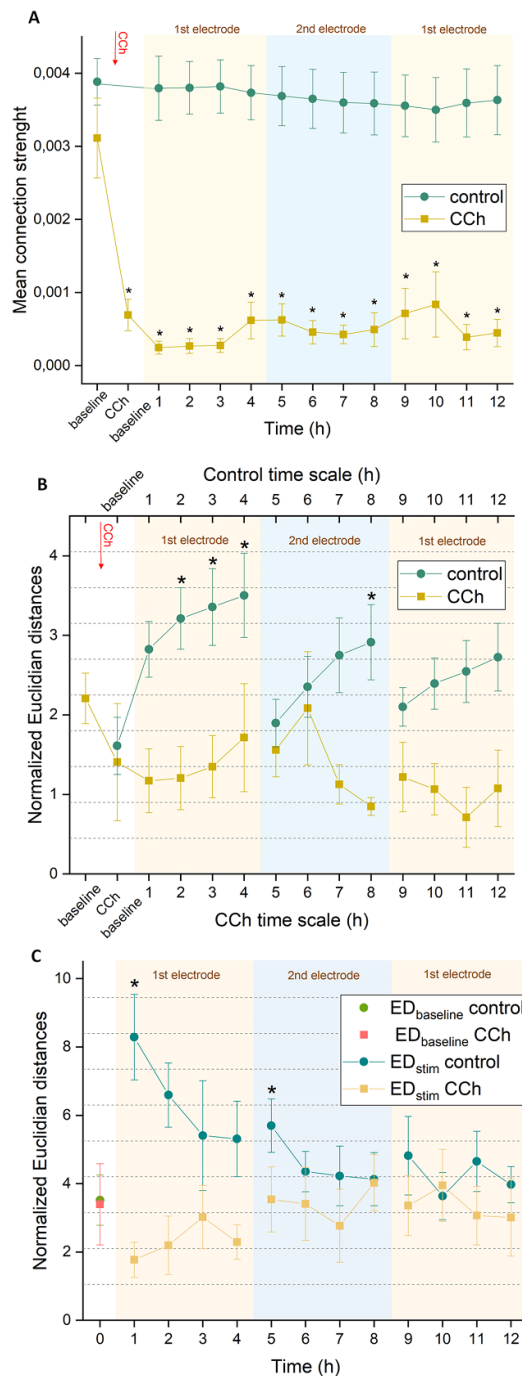
Figure 5. Connectivity changes require high connection strength, low cholinergic input and mainly occur during the first stimulation period in each electrode. (A) Mean strength of control and CCh-treated connections. Baseline values between groups did not differ. Mean connection strength in control cultures did not change during the 12 h procedure. CCh administration (red arrow) reduced the mean connection strength, which remained unaffected throughout experiments. *indicates significant differences; repeated measures ANOVA with Bonferroni correction. (B) Normalized Euclidian distances between connectivity matrices for control (green circles) and CCh-treated cultures (yellow squares). *X*-axes show time scales for CCh-treated cultures (bottom), or control experiments (top). Baseline values did not differ between both groups. Upon stimulation with the first electrode, $ED_{0, norm}$ increased significantly in control cultures. Switching to a second electrode again yielded larger distances between connectivity matrices separated by the first stimulation period, with non-significant differences between subsequent stimulation periods. Returning to stimulation through the first electrode no longer induced significant connectivity changes. We did not observe any significant changes in the $ED_{0, norm}$ of CCh-treated cultures throughout the stimulation protocol. *indicates significant differences; repeated measures ANOVA with Bonferroni correction. (C) Normalized Euclidian distances from the connectivity during baseline ($ED_{baseline}$ for controls in light green and for CCh-treated cultures in red) and from the connectivity before the last stimulation period (ED_{stim} for controls in green and for CCh-treated cultures in yellow). The *x*-axis shows the time scale for both groups, with $t = 0$ corresponding to baseline values before the stimulation protocol. ED_{stim} significantly differs from baseline values in control cultures after the first stimulation period ($ED_{stim}[1]$, control) with the first electrode and after the first stimulation period ($ED_{stim}[5]$, control) with the second electrode. We did not find any significant differences in ED_{stim} after returning to stimulation with the first electrode. No significant changes were observed in ED_{stim} values of CCh-treated cultures. Error bars represent SEM; coloured panels indicate stimulation phases with specific stimulation electrode; *indicates significant differences; repeated measures ANOVA with Bonferroni correction.

differed significantly from $ED_{baseline}$ (repeated measures one-way ANOVA, $p < 0.002$), but $ED_{stim}[2]$, $ED_{stim}[3]$ and $ED_{stim}[4]$ did not. Switching to a second stimulation electrode yielded a significant connectivity change around the first stimulation period ($ED_{stim}[5] > ED_{baseline}$, repeated measures one-way ANOVA, $p < 0.012$), but not around later periods (repeated measures one-way ANOVA, $p > 0.31$). Returning to the first electrode yielded no significant connectivity changes (repeated measures one-way ANOVA, $p > 0.31$). The effect of stimulation was again strikingly different in CCh-treated cultures, in which we did not observe any significant changes in ED_{stim} throughout the duration of the experiment (repeated measures one-way ANOVA, $p > 0.4$).

3.4. Cholinergic activation decreases network excitability

To study the possible effects of carbachol on network excitability, we compared mean SPR strengths in the control group and the CCh-treated group. Cholinergic activation significantly decreased network excitability from $(2 \pm 1) \cdot 10^{-2}$ to $(4 \pm 7) \cdot 10^{-4}$ (Wilcoxon test, $p < 0.02$).

4. Discussion

In this study, we aimed to untangle the role of network bursts and cholinergic input in memory consolidation. Repeated electrical stimulation was applied in cultures with or without cholinergic input, and the consolidation of memory traces was compared between both groups. Increased cholinergic tone transformed activity patterns from burst-dominated into dispersed firing while electrical stimulation induced connectivity changes in cultures bursting spontaneously, but not in carbachol-treated cultures.

4.1. Effect of electrical stimulation on connectivity

First application of low frequency electrical stimulation at one electrode led to substantial changes in network connectivity of spontaneously bursting control cultures, while repetition of the same stimulus did not perpetrate further changes. These observations are in line with a previous study (le Feber *et al* 2015) that applied tetanic stimulation (high-frequency pulse trains at 100 Hz), and confirmed that low frequency stimulation in spontaneously bursting cultures was able to consolidate memory traces. Stimulation at a second electrode again yielded large connectivity changes around the first stimulation period, and non-significant changes around subsequent stimulation periods. This implies that the absence of connectivity changes upon subsequent application of the first stimulus were not due to impeded network plasticity. If stimulation at the second electrode and formation of the second memory trace would erase the memory trace of the first stimulus, a second series of stimuli

at the first electrode would again induce connectivity changes, that subside during subsequent application (le Feber *et al* 2015). However, this did not affect network connectivity, suggesting that the memory trace was still present. The shape of the curves in figure 5(B) are very similar to those obtained with tetanic stimulation (le Feber *et al* 2015).

In contrast, carbachol-treated cultures did not reveal significant changes away from baseline connectivity upon first or subsequent application of the stimulus. We conclude that in the presence of cholinergic input and absence of synchronized bursts, repeated stimulation did not lead to the consolidation of memory traces. This observation agrees with the finding that *in vivo*, SWS—a phase during sleep characterized by low cholinergic input to the cortex—is essential for memory consolidation (Gais and Born 2004, Power 2004, Micheau and Marighetto 2011, Gais and Schönauer 2017).

4.2. Connectivity changes reflect memory trace formation

Previous studies have demonstrated that electrical stimulation can lead to memory trace consolidation within naturally bursting cultures (Marom and Shahaf 2002, Ju *et al* 2015). Nakazawa *et al* (2004) defined four critical features of a memory trace: it must be consolidated in an experience-dependent manner, be specific to the stimulus provided, outlast the period to which a network is exposed to stimulation and it should be reactivated after subsequent presentation of the stimuli that underlined its onset (Nakazawa *et al* 2004). Our results in control cultures directly comply with the first three criteria and indirectly with the last one. Firstly, the connectivity changes we observed occurred upon external stimulation, which can be seen as an experience-dependent interaction. Secondly, stimulation through different electrodes induced different connectivity changes, which implies that changes were specific to the delivered stimulus. Thirdly, connectivity changes induced during the first stimulation at the first electrode were still present after 4 h of stimulation at the second electrode. Finally, the finding that connectivity remained unchanged after presenting again the first stimulus suggests that reactivation of the trace occurred, with no further forces disturbing the established balance. Previous work using tetanic stimulation support these observations (Shahaf *et al* 2008, Kermany *et al* 2010) and report parallel consolidation of memory traces (le Feber *et al* 2015). Memory trace consolidation during systems consolidation is thought to require several hours to days to occur, which is more than the time needed in our experiments. The relatively small size of our network and the simplicity and long duration of our stimuli might have accelerated this process (McKenzie and Eichenbaum 2011).

4.3. Low frequency oscillations are associated with enhanced memory consolidation

Following this line of thought, the observation that stimulation did not induce any connectivity changes in carbachol-treated cultures implies that these networks were unable to consolidate the given cues. This implication is supported by a vast body of literature focusing on the role of ACh and synchronized neural activity in memory consolidation and formation *in vivo* (Axmacher *et al* 2006, Micheau and Marighetto 2011, Atherton *et al* 2015, Miyawaki and Diba 2016, Roumis and Frank 2016, Gais and Schönauer 2017, Mizuseki and Miyawaki 2017, Skelin *et al* 2019). It is generally presumed that increased cholinergic input to the hippocampus in the awake state is necessary for memory formation, while a low cholinergic tone during SWS is required for memory consolidation in the neocortex (Micheau and Marighetto 2011, Gais and Schönauer 2017). Moreover, when memories are acquired during arousal, theta oscillations abound, while during systems consolidation in SWS, synchronized oscillations are thought to induce long-lasting forms of synaptic plasticity, allowing memory consolidation in the neocortex (Axmacher *et al* 2006, Atherton *et al* 2015). In earlier experimental work, sharp-wave ripples (SWRs) were suppressed during sleep, after a memory training task, which impaired spatial learning (Girardeau *et al* 2009), while an increase in sleep SPs and SWRs densities during SWS was reported after a period of intense wordlist learning (Gais and Born 2004). Enhancement of neocortical SOs and SPs by exogenous stimulation has also led to improved memory consolidation (Marshall *et al* 2006, Binder *et al* 2014). Other studies have shown that blocking cholinergic transmission improved consolidation of declarative memory when subjects were tested after a period of SWS (Rasch *et al* 2009) whereas cholinergic activation before SWS induced a deterioration in recalling a previously conducted memory task (Gais and Born 2004). These observations suggest that high ACh levels and the absence of SWRs might facilitate memory encoding but hamper memory consolidation. Our results agree with this latter supposition. Indeed, whereas spontaneously bursting cultures with low cholinergic tone consolidated the given cues, in the presence of cholinergic input and absence of synchronized oscillations we did not observe consolidation. Although our findings seem to be supported by an immense body of work in the realm of memory consolidation and sleep, only few studies actually tested the effects of carbachol administration experimentally (Tateno *et al* 2005, Stamper *et al* 2009, le Feber *et al* 2014). To our knowledge, the present work is the first to combine electrical stimulation and cholinergic activation in dissociated cortical cultures to explore memory consolidation *in vitro*.

4.4. Carbachol reduces network excitability

Carbachol, a synthetic derivative of choline resistant to hydrolysing enzymes such as acetylcholinesterase, persisted in the culture medium throughout the duration of experiments (Stamper *et al* 2009). We used 10 μM CCh, which is within the range of choline concentrations in rodents, is comparable to the estimated ACh concentration in the awake cortex and is equivalent to the desynchronization effect of ACh at this concentration (Tateno *et al* 2005).

Corner and colleagues observed increased bursting and continuous low-level spike activity by acutely adding atropine, a muscarinic antagonist, in neuronal cultures (Corner 2008). A later study showed reduced synchronicity of neuronal firing after carbachol administration (Corner and van der Togt 2012). Greatly enhanced burst activity through muscarinic blockage is in agreement with the observation that carbachol transforms activity patterns from burst dominated into more dispersed firing. Although their work focussed mainly on the role of bursting in neuronal development and maturation, the authors already emphasised the importance of an isolated brain preparation that not only 'sleeps', but that is also capable of displaying the 'desynchronized' firing patterns characteristic of the physiologically aroused neocortex, to study mechanisms underlying SWS-dependent consolidation of learned material through a stimulus-related plasticity protocol (Corner 2008).

Carbachol treatment transformed patterns from burst-dominated into more dispersed firing, which persisted throughout the 15 h recording period. This is in line with earlier work that showed a loss in the regularity and synchronization of activity patterns up to 24 h after CCh administration (10–50 μM) (Tateno *et al* 2005, le Feber *et al* 2014). Similar effects on excitability and activity patterns were found for another mildly excitatory agent, ghrelin, supporting the idea that the effects are not specific to cholinergic input, but more generally result from mild excitation (le Feber *et al* 2014). This switch is thought to be caused by muscarinic receptor activation (Drever *et al* 2011). Earlier studies showed that the size of excitatory post-synaptic potentials in several cortical synapses was reduced by muscarinic receptor activation (Gil *et al* 1997) and that most neurons in hippocampal cultures showed a marked reduction in the magnitude of evoked post synaptic potentials (Segal 1983). In the current study, network activity increased upon CCh administration and network excitability (as quantified by average SPR) decreased.

Several mechanisms, including synaptic scaling, activation of the inhibitory system, and short-term synaptic depression, may reduce network excitability. Homeostatic synaptic scaling is a form of plasticity that stabilizes total network firing, with a time constant in the order of a day (Turrigiano 2010). As

we observed an immediate increase in network activity and an instantaneous decrease in network excitability, it is improbable that synaptic scaling is the responsible mechanism (Vinson and Justice 1997, van Pelt *et al* 2005). Activation of inhibitory neurons in turn would be translated into a rapid activity decrease upon CCh administration, outweighing the excitatory effect of CCh. The immediate increase in network activity contradicts induced inhibition as a possible mechanism. It is more plausible that reduced network excitability resulted from increased short-term depression of recurrent excitatory synapses (le Feber *et al* 2014) due to increased synaptic activation (Zucker and Regehr 2002). Short-term depression is caused by depletion of neurotransmitter, and thus occurs presynaptically. This view agrees with earlier works that observed a suppressive effect of ACh on the spread of excitation in the visual cortex presynaptically (Kimura *et al* 1999), and a reduction of postsynaptic potentials in hippocampal cultures to be presynaptically mediated (Segal 1983). The notion of reduced excitability was confirmed by the effect of carbachol on stimulus responses. Both tetanic and low-frequency electrical stimulation can trigger network bursts of relatively many action potentials (Lindner *et al* 2017, Bell *et al* 2018). Based on earlier work, it has been hypothesized that these evoked network bursts are needed to induce connectivity changes (Minati *et al* 2010, le Feber *et al* 2015, Lindner *et al* 2017). During baseline, CCh and control networks reacted similarly to low-frequency electrical stimulation, with evoked network bursts shortly after most stimulus pulses. CCh-treated cultures were no longer able to self-generate synchronized bursting patterns. Activation of a few neurons near the stimulation electrode was still possible after CCh administration, but apparently, network wide induced activity is required for the induction of memory traces. This probably requires sufficiently high network excitability, otherwise low frequency pulses cannot activate the entire network, and the stimuli impose insufficiently strong forces away from the current equilibrium.

4.5. Efficacy of electrical stimulation

Network responses to electrical stimulation in CCh-treated and control cultures were quite similar in shape, although stimulus response curves in CCh-treated cultures showed increased uncorrelated background activity before and after stimulus onset. This is in line with the increased offset in CFP curves, which reflects an increase in uncorrelated background activity. The mean area under the PSTH curves was significantly smaller in CCh-treated cultures than in control cultures but did not significantly change between stimulation periods in either group. This excludes the possibility that the vanishing effect of

repeated stimulation on connectivity was related to changing efficacy of stimulation.

4.6. Study limitations

Dissociated cortical cultures are still simplified models of the real *in vivo* architecture of the brain. Declarative memory formation, consolidation and retrieval are complex phenomena involving multiple structures, including the hippocampus, the neocortex, the amygdala and the entorhinal cortex. Our study focussed mainly on memory consolidation in the cortex, as to fully mimic memory formation would require more complex models including hippocampal networks.

Memory consolidation was inferred from connectivity changes induced by electrical stimulation, but memory retrieval was not addressed. Still, the observation that a short stimulus triggers a response that is encoded in network connectivity is in agreement with other studies reporting recollection of entire memory patterns from partial cue presentation, a process known as pattern recollection in the hippocampus (Marr 1971, Hasselmo *et al* 1995, Nakazawa *et al* 2002, Jo *et al* 2007).

The number of cultures used in this study was limited (8 CCh-treated networks and 10 controls, amounting for a total of 18 low-frequency stimulated cultures). However, effects in different experiments were very comparable, suggesting that both groups were sufficiently large to come to solid conclusions. Earlier studies assessing learning (Shahaf and Marom 2001) and memory in cultured neural networks (le Feber *et al* 2015) used comparable sample sizes.

Memory acquisition, consolidation, and recollection are thought to occur in a relatively sequential order, with memories acquired during the awake state and replayed and consolidated during SWS (Power 2004, Nadel *et al* 2012). In our study, each culture was assigned to a different group, either control (mimicking the SWS state) or CCh-treatment (mimicking the awake state), and so networks were never assessed under both pharmacological conditions.

5. Conclusion

Synchronized bursting patterns of unperturbed dissociated cortical cultures can be disrupted by cholinergic activation. We conclude that spontaneously bursting networks of dissociated cortical neurons are able to memorize given cues, whereas high cholinergic tone, the absence of synchronized patterns, and low network excitability impede memory consolidation. These results together corroborate that cholinergic activation debilitates memory consolidation, possibly through decreased network excitability. In this view, network bursts or SWS oscillations may merely reflect the intrinsic premise to enable the consolidation of memory traces: high network excitability.

Data availability statement

Acknowledgment

Author contributions

Conceptualization, I D and J lF; Methodology, I D and J l F; Software, I D and J l F; Formal Analysis, I D, M L, and J l F; Investigation, I D; Resources, M R L and G C H; Writing—Original Draft, I D and J l F; Writing—Review & Editing, I D, M R L, M L, G C H, R v W, and J l F.

ORCID iDs

Inês Dias ⓘ https://orcid.org/0000-0002-5404-4506
Joost le Feber ⓘ https://orcid.org/0000-0002-0605-1437

References

Atherton L A, Dupret D and Mellor J R 2015 Memory trace replay: the shaping of memory consolidation by neuromodulation *Trends Neurosci.* **38** 560–70

Axmacher N *et al* 2006 Memory formation by neuronal synchronization *Brain Res. Rev.* **52** 170–82

Baltz T, de Lima A D and Voigt T 2010 Contribution of GABAergic interneurons to the development of spontaneous activity patterns in cultured neocortical networks *Front. Cell Neurosci.* **4** 1–15

Bell T *et al* 2018 Functional neurochemical imaging of the human striatal cholinergic system during reversal learning *J. Neurosci.* **47** 1184–93

Binder S *et al* 2014 Brain stimulation transcranial slow oscillation stimulation during sleep enhances memory consolidation in rats *Brain Stimul.* **7** 508–15

Bologna L L *et al* 2010 Investigating neuronal activity by SPYCODE multi-channel data analyzer *Neural. Netw.* **23** 685–97

Colangelo C *et al* 2019 Cellular, synaptic and network effects of acetylcholine in the neocortex *Front. Neural. Circuits* **13** 1–24

Corner M A 2008 Spontaneous neuronal burst discharges as dependent and independent variables in the maturation of cerebral cortex tissue cultured *in vitro*: a review of activity-dependent studies in live 'model' systems for the development of intrinsically generated bioel *Brain Res. Rev.* **59** 221–44

Corner M and van der Togt C 2012 No phylogeny without ontogeny—a comparative and developmental search for the sources of sleep-like neural and behavioral rhythms *Neurosci. Bull.* **28** 25–38

Dranias M R *et al* 2013 Short-term memory in networks of dissociated cortical neurons *J. Neurosci.* **33** 1940–53

Drever B D, Riedel G and Platt B 2011 The cholinergic system and hippocampal plasticity *Behav. Brain Res.* **221** 505–14

Fardet T *et al* 2018 Understanding the generation of network bursts by adaptive oscillatory neurons *Front. Neurosci.* **12** 1–14

Fries P 2015 Rhythms for cognition: communication through coherence *Neuron* **88** 220–35

Gais S and Born J 2004 Low acetylcholine during slow-wave sleep is critical for declarative memory consolidation *Proc. Natl Acad. Sci.* **101** 2140–4

Gais S and Schönauer M 2017 Untangling a cholinergic pathway from wakefulness to memory *Neuron* **94** 696–8

Gil Z, Connors B W and Amitai Y 1997 Differential regulation of neocortical synapses by neuromodulators and activity *Neuron* **19** 679–86

Girardeau G *et al* 2009 Selective suppression of hippocampal ripples impairs spatial memory *Nat. Neurosci.* **12** 1222–3

Hasselmo M E 1999 Neuromodulation: acetylcholine and memory consolidation *Trends Cogn. Sci.* **3** 351–9

Hasselmo M E, Schnell E and Barkai E 1995 Dynamics of learning and recall at excitatory recurrent synapses and cholinergic modulation in rat hippocampal region CA3 *J. Neurosci.* **15** 5249–62

Jo Y S *et al* 2007 The medial prefrontal cortex is involved in spatial memory retrieval under partial-cue conditions *J. Neurosci.* **27** 13567–78

Ju H *et al* 2015 Spatiotemporal memory is an intrinsic property of networks of dissociated cortical neurons *J. Neurosci.* **35** 4040–51

Kermany E *et al* 2010 Tradeoffs and constraints on neural representation in networks of cortical neurons *J. Neurosci.* **30** 9588–96

Kimura F, Fukuda M and Tsumoto T 1999 Acetylcholine suppresses the spread of excitation in the visual cortex revealed by optical recording: possible differential effect depending on the source of input *Eur. J. Neurosci.* **11** 3597–609

le Feber J *et al* 2007 Conditional firing probabilities in cultured neuronal networks: a stable underlying structure in widely varying spontaneous activity patterns *J. Neural. Eng.* **4** 54–67

le Feber J *et al* 2015 Repeated stimulation of cultured networks of rat cortical neurons induces parallel memory traces *Learn. Mem.* **22** 594–603

le Feber J, Tzafi Pavlidou S, Erkamp N, van Putten MJAM and Hofmeijer J 2016 Progression of neuronal damage in an *in vitro* model of the ischemic penumbra *PLoS One* **11** 1–19

le Feber J *et al* 2017 Loss and recovery of functional connectivity in cultured cortical networks exposed to hypoxia *J. Neurophysiol.* **118** 394–403

le Feber J *et al* 2018 Evolution of excitation–inhibition ratio in cortical cultures exposed to hypoxia *Front. Cell Neurosci.* **12** 1–10

le Feber J, Stegenga J and Rutten W L C 2010 The effect of slow electrical stimuli to achieve learning in cultured networks of rat cortical neurons *PLoS One* **5** 1–8

le Feber J, Stoyanova I I and Chiappalone M 2014 Connectivity, excitability and activity patterns in neuronal networks *Phys. Biol.* **11** 1–11

Lewicki M S 1998 A review of methods for spike sorting: the detection and classification of neural action potentials *Network* **9** 53–78

Lindner M *et al* 2017 *In vivo* functional neurochemistry of human cortical cholinergic function during visuospatial attention *PLoS One* **12** 1–16

Lisman J E 1997 Bursts as a unit of neural information: making unreliable synapses reliable *Trends Neurosci.* **20** 38–43

Marom S and Shahaf G 2002 Development, learning and memory in large random networks of cortical neurons: lessons beyond anatomy *Q. Rev. Biophys.* **35** 63–87

Marr D 1971 Simple memory: a theory for archicortex *Phil. Trans. R. Soc.* B **262** 23–81

Marshall L *et al* 2006 Boosting slow oscillations during sleep potentiates memory *Nature* **444** 610–3

McKenzie S and Eichenbaum H 2011 Consolidation and reconsolidation: two lives of memories? *Neuron* **71** 224–33

Micheau J and Marighetto A 2011 Acetylcholine and memory: a long, complex and chaotic but still living relationship *Behav. Brain Res.* **221** 424–9

Miles R and Wong R 1983 Single neurons can initiate synchronized population discharge in the hippocampus *Nature* **306** 371–3

Minati L *et al* 2010 Quantitation of normal metabolite concentrations in six brain regions by *in-vivo* 1 H-MR spectroscopy *J. Med. Phys.* **35** 154–63

Miyawaki H and Diba K 2016 Regulation of hippocampal firing by network oscillations during sleep *Curr. Biol.* **26** 893–902

Mizuseki K and Miyawaki H 2017 Hippocampal information processing across sleep/wake cycles *Neurosci. Res.* **118** 30–47

Nadel L *et al* 2012 Memory formation, consolidation and transformation *Neurosci. Biobehav. Rev.* **36** 1640–5

Nakazawa K *et al* 2002 Requirement for hippocampal CA3 NMDA receptors in associative memory recall *Science* **297** 211–8

Nakazawa K *et al* 2004 NMDA receptors, place cells and hippocampal spatial memory *Nat. Rev. Neurosci.* **5** 361–72

Pasquale V *et al* 2008 Self-organization and neuronal avalanches in networks of dissociated cortical neurons *Neuroscience* **153** 1354–69

Power A E 2004 Slow-wave sleep, acetylcholine, and memory consolidation *Proc. Natl Acad. Sci. USA* **101** 1795–6

Queenan B N *et al* 2017 On the research of time past: the hunt for the substrate of memory *Ann. New York Acad. Sci.* **1396** 108–25

Rasch B, Gais S and Born J 2009 Impaired off-line consolidation of motor memories after combined blockade of cholinergic receptors during REM sleep-rich sleep *Neuropsychopharmacology* **34** 1843–53

Roumis D K and Frank L M 2016 Hippocampal sharp-wave ripples in waking and sleeping states demetris *Curr. Opin. Neurobiol.* **35** 6–12

Saberi-Moghadam S *et al* 2018 *In vitro* cortical network firing is homeostatically regulated: a model for sleep regulation *Sci. Rep.* **8** 6297

Segal M 1983 Rat hippocampal neurons in culture: responses to electrical and chemical stimuli *J. Neurophysiol.* **50** 1249–64

Shahaf G *et al* 2008 Order-based representation in random networks of cortical neurons *PLoS Comput. Biol.* **4** e1000228

Shahaf G and Marom S 2001 Learning in networks of cortical neurons *J. Neurosci.* **21** 8782–8

Skelin I, Kilianski S and McNaughton B L 2019 Hippocampal coupling with cortical and subcortical structures in the context of memory consolidation *Neurobiol. Learn. Mem.* **160** 21–31

Stamper R, Lieberman M and Drake M 2009 Cholinergic drugs *Becker-Shaffer Diagnosis and Therapy of the Glaucomas* 8th edn (Maryland Heights, MO: Mosby) pp 420–30

Steriade M and Timofeev I 2003 Neuronal plasticity in thalamocortical review networks during sleep and waking oscillations *Neuron* **37** 563–76

Sukiban J *et al* 2019 Evaluation of spike sorting algorithms: application to human subthalamic nucleus recordings and simulations *Neuroscience* **414** 168–85

Tateno T, Jimbo Y and Robinson H P C 2005 Spatio-temporal cholinergic modulation in cultured networks of rat cortical neurons: evoked activity *Neuroscience* **134** 425–37

Teppola H, Aćimović J and Linne M L 2019 Unique features of network bursts emerge from the complex interplay of excitatory and inhibitory receptors in rat neocortical networks *Front. Cell Neurosci.* **13** 1–22

Turrigiano G G 2010 The self-tuning neuron: synaptic scaling of excitatory synapses *Cell* **135** 422–35

Turrigiano G G and Nelson S B 2000 Hebb and homeostasis in neuronal plasticity *Curr. Opin. Neurobiol.* **10** 358–64

van Pelt J *et al* 2005 Dynamics and plasticity in developing neuronal networks *in vitro Prog. Brain Res.* **147** 173–88

van Pelt J, Wolters P S, Corner M A, Rutten W L C and Ramakers G J A 2004 Long-term characterization of firing dynamics of spontaneous bursts in cultured neural networks *IEEE Trans. Biomed. Eng.* **51** 2051–62

Vinson P N and Justice J B Jr 1997 Effect of neostigmine on concentration and extraction fraction of acetylcholine using quantitative microdialysis *J. Neurosci. Methods* **73** 61–67

Wagenaar D A *et al* 2005 Controlling bursting in cortical cultures with closed-loop multi-electrode stimulation *J. Neurosci.* **25** 680–8

Wagenaar D, Demarse T B and Potter S M 2005 MeaBench: a toolset for multi-electrode data acquisition and on-line analysis *2nd Int. IEEE EMBS Conf. on Neural Engineering* pp 518–21

Wagenaar D, Nadasdy Z and Potter S M 2006 Persistent dynamic attractors in activity patterns of cultured neuronal networks *Phys. Rev.* E **73** 51907–15

Yger P and Gilson M 2015 Models of metaplasticity: a review of concepts *Front. Comput. Neurosci.* **9** 1–14

Zucker R S and Regehr W G 2002 Short-term synaptic plasticity *Annu. Rev. Physiol.* **64** 355–405